HAL open science

Evaporating droplets tracking by holographic high speed video in turbulent flow

Loïc Méès, Thibaut Tronchin, Nathalie Grosjean, Jean-Louis Marié, Corinne Fournier

To cite this version:

Loïc Méès, Thibaut Tronchin, Nathalie Grosjean, Jean-Louis Marié, Corinne Fournier. Evaporating droplets tracking by holographic high speed video in turbulent flow. 18th International Symposium on applications of laser techniques to fluid mechanics, Jul 2016, Lisbonne, Portugal. hal-02404953

HAL Id: hal-02404953

https://hal.science/hal-02404953v1

Submitted on 11 Dec 2019

HAL is a multi-disciplinary open access archive for the deposit and dissemination of scientific research documents, whether they are published or not. The documents may come from teaching and research institutions in France or abroad, or from public or private research centers.

L'archive ouverte pluridisciplinaire **HAL**, est destinée au dépôt et à la diffusion de documents scientifiques de niveau recherche, publiés ou non, émanant des établissements d'enseignement et de recherche français ou étrangers, des laboratoires publics ou privés.

Evaporating droplets tracking by holographic high speed video in turbulent flow

Loïc Méès[1*], Thibaut Tronchin[1], Nathalie Grosjean[1], Jean-Louis Marié[1] and Corinne Fournier[2]
1: Laboratoire de Mécanique des Fluides et d'Acoustique, UMR CNRS 5509, Ecole Centrale de Lyon, Université de Lyon, France
2: Laboratoire Hubert Curien, UMR CNRS 5516, Université Jean Monnet, Université de Lyon, France
* Correspondent author: loic.mees@ec-lyon.fr

Keywords: Holography, Inverse Problem, Droplet Evaporation, Turbulent flow

ABSTRACT

The evaporation rate of diethyl ether droplets dispersing in a Homogeneous and isotropic (HI) turbulence is measured by following droplets along their trajectory. Measurements are performed at ambient temperature and pressure by using in-line digital holography. The holograms of droplets are recorded with a single high-speed camera (3kHz) and reconstructed with an inverse problems approach (IPA). IPA provides a measurement of droplet size and location accurate enough to follow the dynamic of the droplets in 3 dimensions as well as their instantaneous evaporation rate though their size evolution. In addition, the thermal-vapor concentration wakes developing around the droplets are visible on holograms. It is found that these wakes when reconstructed using a classical back light propagation method are aligned with the relative Lagrangian velocity seen by the droplets at each time. The relative velocity can be calculated from the droplets equation of motion and the positions and diameter measured by holography and IPA processing, when the orientation of the wake is independently deduced from the phase retrieval of the vapor wake. Droplets trajectories and time evolution of diameter and relative velocity are presented. In a number of cases, the evaporation rate of the droplets changes along the trajectory and deviates from that calculated with a standard film model, showing that turbulence may influence significantly the evaporation process.

---

1. Introduction

In many practical situations droplets vaporize in turbulent flow. It is then of primary importance to know whether or not turbulence influences evaporation (Birouk and Gokalp 2006; Reveillon and Demoulin 2007). The most physically relevant approach to investigate this question is to adopt a Lagrangian point of view and measure the phase change of the droplet by following its diameter evolution along its trajectory. This is the objective that we aim to achieve with the experiments presented here. Diethyl Ether droplets are released in a homogeneous isotropic and strong turbulence produced by synthetic jets as described in (Goepfert et al 2010). One interest of this situation is that the parameters of the turbulence are well controlled. The Lagrangian tracking method that has been chosen is in-line digital holography associated with an Inverse Problem Approach (IPA). This approach provides the highly accurate measurement of droplet

size and position required for both droplet tracking and evaporation rate measurement at a relatively large distance. The paper is organized as follow. After this introduction, section 2 gives a short description of the holographic setup. The hologram processing is described in section 3. Holograms are first processed using an inverse problem approach (IPA) to detect the droplet and to measure their 3D position and diameter. A second reconstruction process, based on a standard back light propagation method is then apply to the residual images to reconstruct the wake of vapor around the droplets. Results obtained on a sample of droplets trajectories are presented and discussed in section 4, where measured evaporation rates are compare to those deduced from a simple evaporation/condensation model. Section 5 is a conclusion.

2. Holographic setup

Fig.1 provides a schematic of the optical set-up. It consists of a diverging beam illuminating the measurement volume and a CMOS sensor of a high speed camera (V611 phantom, 1280x800 pixel of 20µm). The measurement volume is located at the intersection of synthetic jets generated by six woofers (only four are presented in the figure for convenience) resulting in a homogeneous and isotropic turbulence (HIT) in the whole measurement volume. This measurement volume is determined by the source point (focal point of the laser) CMOS sensor distance and size (25.6x16.0 mm^2) and limited in z direction to superimposed with the volume where HIT is ensured. Its dimensions are approximately 16x10x50 mm^3. The mean flow velocity, the turbulence fluctuations and the integral length scale of the HIT are of the order of 0.03 ms^{-1}, 0.8 ms^{-1} and 49 mm respectively. The divergence of the beam leads to a magnification ratio *m* of the holograms which depends on the droplet z coordinate following

$$m(z)=\frac{z_s}{z_s-(z_0+z)}$$

Where z_s is the distance between the CMOS sensor and the light source S, z_0 the distance between the CMOS sensor and the center O of the measurement volume and the coordinate system. The magnification factor has been deduced from calibration by using a linear scale glass reticle (Edmunds Optics, 62 – 252), following the same procedure as in Marié et al (2014). In the present configuration, the magnification ratio is about 1.544 for z=0 and it varies between 1.51 and 1.58 in the measurement volume, corresponding to $z_s=1778\,mm$ and $z_0=626.5\,mm$.

The droplets are generated by a piezoelectric MJ-AT-01 MicroFab Technologies jetting device, equipped with a 60 µm orifice diameter glass capillary. Unlike in Chareyron et al (2012); Marié et al (2014) where the "drop on demand" mode was used, it is operated in continuous droplet jet-mode. The ether jet created at the capillary exit by a syringe pump is disrupted and delivers droplets of approximately 1.8 times the orifice diameter (Lee 2003), that is about 110 µm, with an

initial velocity of the order of 2 m.s^{-1}. Injection parameters are adjusted to allow a sufficient number of droplets enters the measurement volume. The injector positioning is critical as the droplets must enter the volume before completely evaporating, the injector should not be to close to the volume and modify the turbulence properties and the droplets must be "trapped" in the HIT volume.

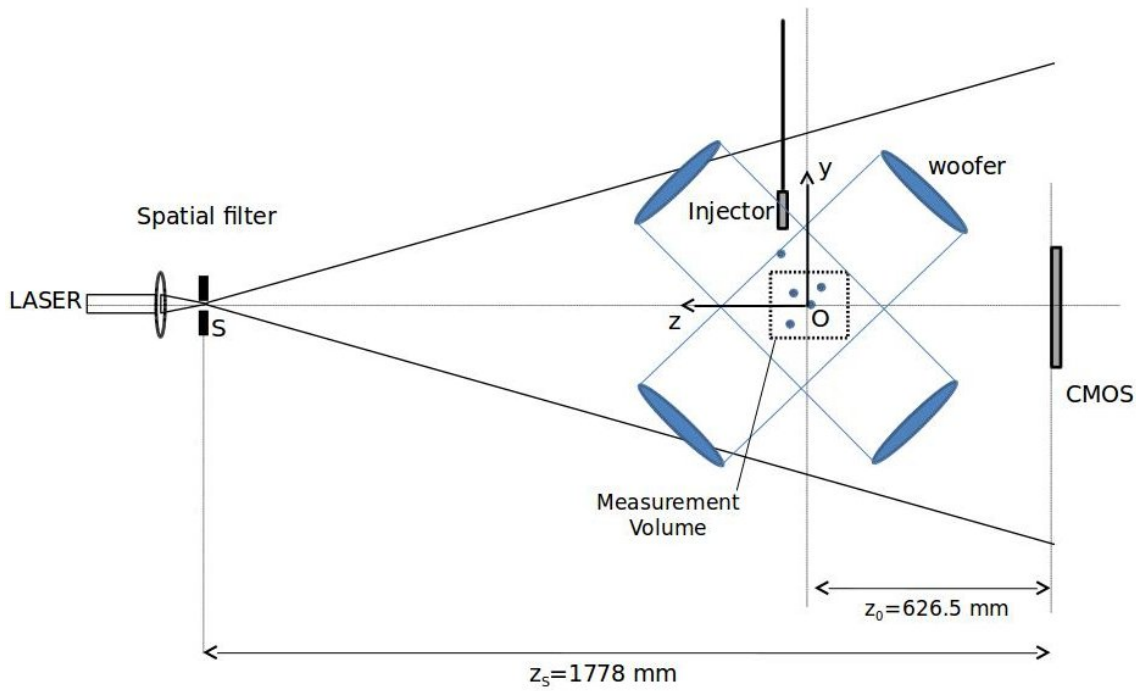

Fig.1 Experimental set-up.

3. Hologram processing

Time sequences (videos) of droplets holograms are recorded under the conditions described above at 3kHz. For each run, a background correction is applied, the background image being calculated by averaging on the whole sequence. Fig. 2 shows an example of droplets hologram after the background correction. Droplets holograms consist of circular fringes resulting from interferences between the droplet diffraction pattern and the reference beam which is the illuminating beam it-self in the in-line configuration here considered. A wake, attached to the hologram is also clearly visible in Fig 2, for the droplet near the image center in particular. It results from the vapor wake due to evaporation and the associated refractive index gradient in the gas phase surrounding the droplet as discussed in Méès et al (2013). The wake will be considered later, it can be first ignored (Seifi et al, 2013) to estimate droplet position and diameter using an 'inverse problem' approach (IPA). This procedure is based on the minimization of the

difference between the recorded hologram and a model hologram, based on Fraunhoffer diffraction of an opaque disk. The IPA method is described in Soulez et al (2007a) and Soulez et al (2007b) and has been successfully applied in Chareyron et al (2012), Seifi et al (2013) and Marié et al (2014). The Fraunhoffer diffraction model is accurate enough in such a configuration (at large distance) to describe a droplet hologram (without wake), using if necessary a mask in the center part of the hologram where the wake influence is larger. IPA was preferred to a standard back light propagation procedure to extract the coordinates x,y,z and the diameter of the droplets because the model hologram intrinsically takes into account truncation and low spatial resolution of the sensor which are significant sources of error and low accuracy measurements. The accuracy expected for 60 μm diameter water droplets dispersing in the turbulence under the same operating conditions as here, has typically be estimated to less than 1 μm on diameter, 3 μm (about one tenth of pixel size) on the transverse positions (parallel to the sensor) and about 60 μm (one diameter) on depth z (Chareyron et al 2012).

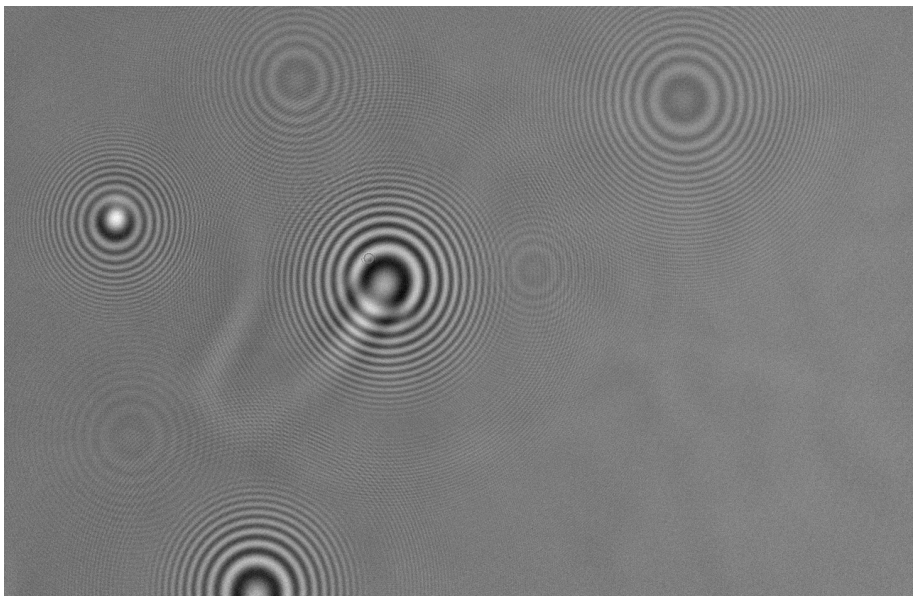

Fig 2 Droplets hologram after background correction.

The minimization procedure applied to the hologram of fig. 2 leads to an estimation of *(x,y,z)* coordinates and diameter *d* of a first droplet, that is located about the center of the image. Then, the corresponding best fit model hologram can be subtracted from the image to obtain a residual image as shown in fig 3. After the subtraction, IPA algorithm can be applied again to detect the next droplet an so on.

In this paper, the residual image is further process to extract information on the vapor wake around the droplets. We assume that gray scale variations around the droplet in the residual image of Fig 3 (near the image center) is only due to the vapor wake generated by the droplet

evaporation. In other words, we assume purely additive contributions of the droplet and the vapor to the hologram and we assume that the IPA procedure has provided the exact parameter (x,y,z,d) describing the droplet alone. The wake image of the residual image is then considered as a phase object hologram and it is phase retrieved using a standard back light propagation method to obtain the image shown in Fig 4. The distance z of reconstruction is that obtained by IPA. Note also that a threshold as been applied to fig 4 to remove the twin image noise associated to standard reconstruction methods. This phase retrieval image provides information on the vapor wake, and its evolution in time when considering a whole sequence of holograms. To be more specific, the retrieved phase depends on the 2D projection along direction z of the refractive index field which depends itself on vapor concentration and temperature. As the droplets trajectories and the flow characteristics are 3D, the extraction of quantitative information on vapor wake is not a small matter. However, the 2D orientation of the wake projection in the *(x,y)* plane is easy extracted from the image, providing a 2D information on relative velocity, the gas flow velocity "viewed" by the droplet.

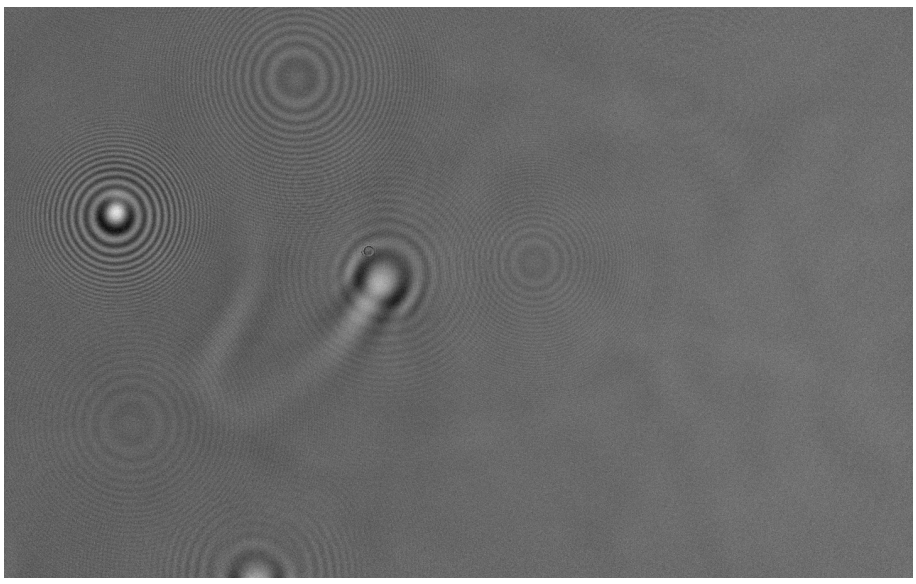

Fig 3 Residual image. Hologram of fig 2 after best fit model subtraction.

Sequences of hologram were thus processed following different step ad follow :

- Background correction of each image of the sequence.
- IPA measurement of (x,y,z,d) for each droplet and image and magnification ratio application.
- Trajectory reconstruction from (x,y,z,d) results (using a nearest-neighbor criteria)
- IPA residual image sequence construction for each droplet trajectory.
- Phase retrieval in the droplet plan from IPA residual images.

- Extraction of the 2D wake orientation along the trajectory.

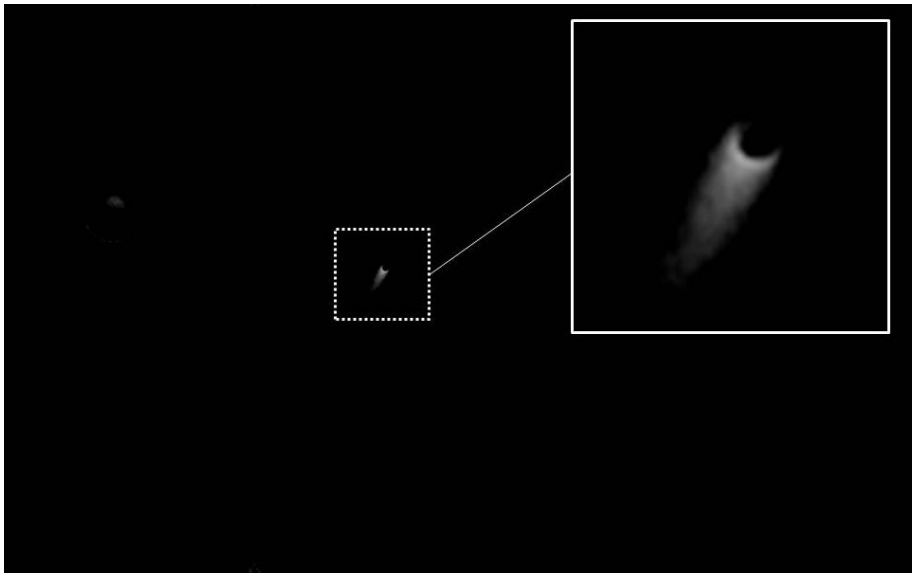

Fig 4 Phase retrieval image, calculated from the residual image presented in fig. 3 by using a standard back light propagation method.

4. Results and discussion

The main objective of this work is to determine whether or not turbulence influences droplets evaporation. Up to now, a few trajectories have been recorded and processed following the procedure described above.

Fig 5 shows the evolution of two typical droplets diameter along there trajectories. The square of diameter evolution with time is compared to that calculated with the simple evaporation/condensation model validated in case of free falling Ether droplets. The model is that described in Marié et al (2014). It takes into account the condensation water from humid air at the droplet surface whose influence can not be neglected. The inputs are the initial size and velocity of the droplet deduced from the first images IPA processing, the initial droplet temperature, and ambient temperature and humidity rate. Humidity rate and room temperature are measured for each run. In this experiment the initial droplet temperature is unknown but it can be set arbitrarily, as the system converge to an equilibrium state after a few time step. In the presented results, the simulation is run once a time with an arbitrary value to determine an equilibrium temperature used in a second run. Another difference between the present simulations and those presented in Marié et al (2014) is that the relative velocity is not constant as for free falling. But the Lagrangian relative velocity is deduced from the IPA measurements (x,y,z,d) versus time and the droplet equation of motion. It requires that the main forces acting

on the droplets reduce to the gravity and drag force, in which case their motion is described by an equation of the form (see for instance Michaelides (2006))

$$\frac{du_d}{dt}=\left(1-\frac{1}{\gamma}\right)g+\frac{3C_D(\mathrm{Re}_d)}{4d\gamma}|u-u_d|(u-u_d) \tag{1}$$

where γ is the density ratio ρ_l/ρ_g between liquid and gas, u_d the droplet velocity , u the gas velocity and Re_d the Reynolds number based on the droplet diameter and the relative velocity $u_r=u-u_d$. This form is justified because the droplets are heavier than the gas, have a size comparable to the Kolmogorov length scale *(0.15 mm)* and do not interact during evaporation, since their concentration is low. The Diethyl Ether droplets having a Reynolds number typically in the range $0\leq\mathrm{Re}_d\leq 10$ the drag coefficient is estimated by the correlation proposed by Clift for this case (Clift et al 1978)

$$C_D(\mathrm{Re}_d)=\frac{24}{\mathrm{Re}_d}\left(1+\beta\,\mathrm{Re}_d^{\alpha}\right) \tag{2}$$

where $\beta=0.1935$ and $\alpha=0.6305$. The unknown Lagrangian relative velocity norm u_r is then inferred by solving the equation obtained by summing the square of the projections of equation (1) along the three directions of the holographic set-up

$$\tau_d^2\left(\dot{u}_{dx}^2+(\dot{u}_{dy}-g)^2+\dot{u}_{dz}^2\right)=u_r^2(1+\beta\,\mathrm{Re}_d^{\alpha})^2 \tag{3}$$

Where $\tau_d=\rho_l d^2/18\mu_g$ and notation $\dot{u}_i$ stands for the derivative of u_i . In practice, τ_d , $\dot{u}_{dx}^2$, $\dot{u}_{dy}^2$ and $\dot{u}_{dz}^2$ are calculated at each time step from the reconstructed trajectory and the measured diameter. Once u_r is determined, Re_d is known and the three components of the relative velocity can be readily deduced from the 3 projections of equation (1).

Fig 5 it can be seen that the simulated time evolutions, including the calculated relative velocity remain very close to the d^2 law which predict a linear evolution of diameter square with time. The experimental result is also very close to this law for droplet 1 but not for droplet 2. More generally, such behavior is observed for about one third of the trajectory recorded and processed until now. Droplet 2 does not evaporate regularly with strong variations of the evaporation rate.

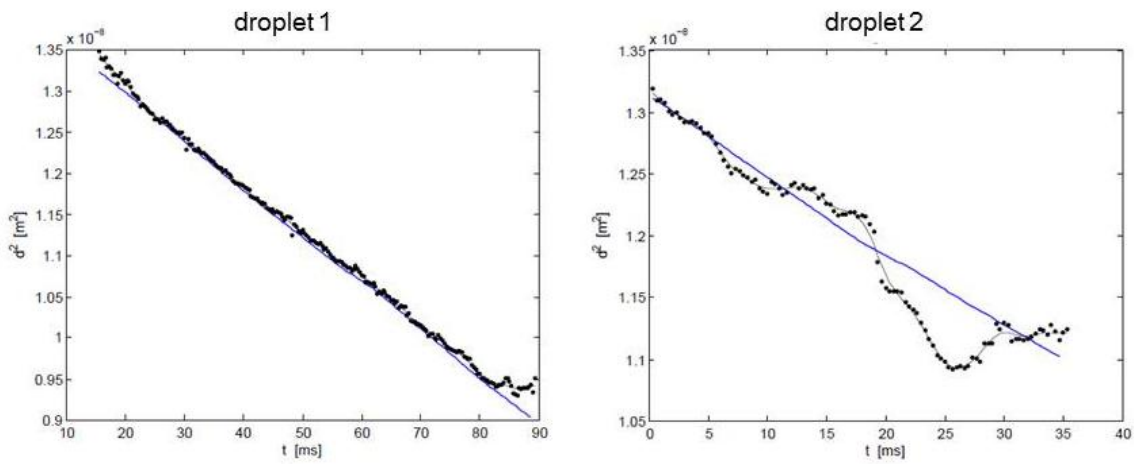

Fig 5 Two typical examples of droplet diameter evolution (diameter square versus time in black) extracted from IPA processing of high speed hologram sequences. Droplet 1 show a similar behavior as observed in free falling condition and agree with the simple evaporation/condensation droplet. Droplet 2 evaporation rate is clearly influenced by the surrounding turbulent flow.

Fig 6 shows a sample of holograms and phase retrieval images extracted from droplet 2 trajectory. The (x,y) projection of the calculated relative velocity (green arrow) and wake orientation (white dashed line) are compared, showing a very good agreement. However, the wake does not realign instantaneously with the relative velocity, but with a certain time delay that corresponds to the response time τ_w of the wake to changes in ur_{xy} direction. This appears in Fig. 7 where the time evolution of the angles of θ_{wxy} the wake axis and of θ_{urxy} the ur_{xy} direction in the (x,y) plane fro droplet 2 are plotted. τ_w can be estimated assuming that θ_{wxy} responds linearly to θ_{urxy} variations as

$$\frac{d\theta_{urxy}}{dt} = \frac{\theta_{urxy} - \theta_{wxy}}{\tau_w} \tag{4}$$

In this example, τ_w = 0.4 ms is the relaxation that ensure the best match between between eq.(4) and the phase retrieved wake angle. The good accordance between the two angles is similar for all the tested trajectories with relaxation time τ_w varying between 0.3 and 1.0 ms. This evidences that droplets positions and diameter measurements and resulting velocities are accurate enough to reproduce well the trajectory and the overall consistency of measurements, including IPA and phase retrieval processing.

The question of the mechanisms responsible for the evaporation rates fluctuations is still open. These fluctuations are often associated with sudden variations of the relative velocity, in amplitude and orientation but no clear dependence as been identified yet. It can be noted

however that rapid decreasing in droplets diameter are generally preceded by a plateau, a short time during which evaporation slow down or nearly stopped. These events seem to coincide with sudden vapor releases clearly visible in fig. 6 at time t=17 and 24 ms. These observations suggest that evaporation rate fluctuations could be related to vapor accumulation around the droplets and sudden sweeping wind but further investigations are definitely required.

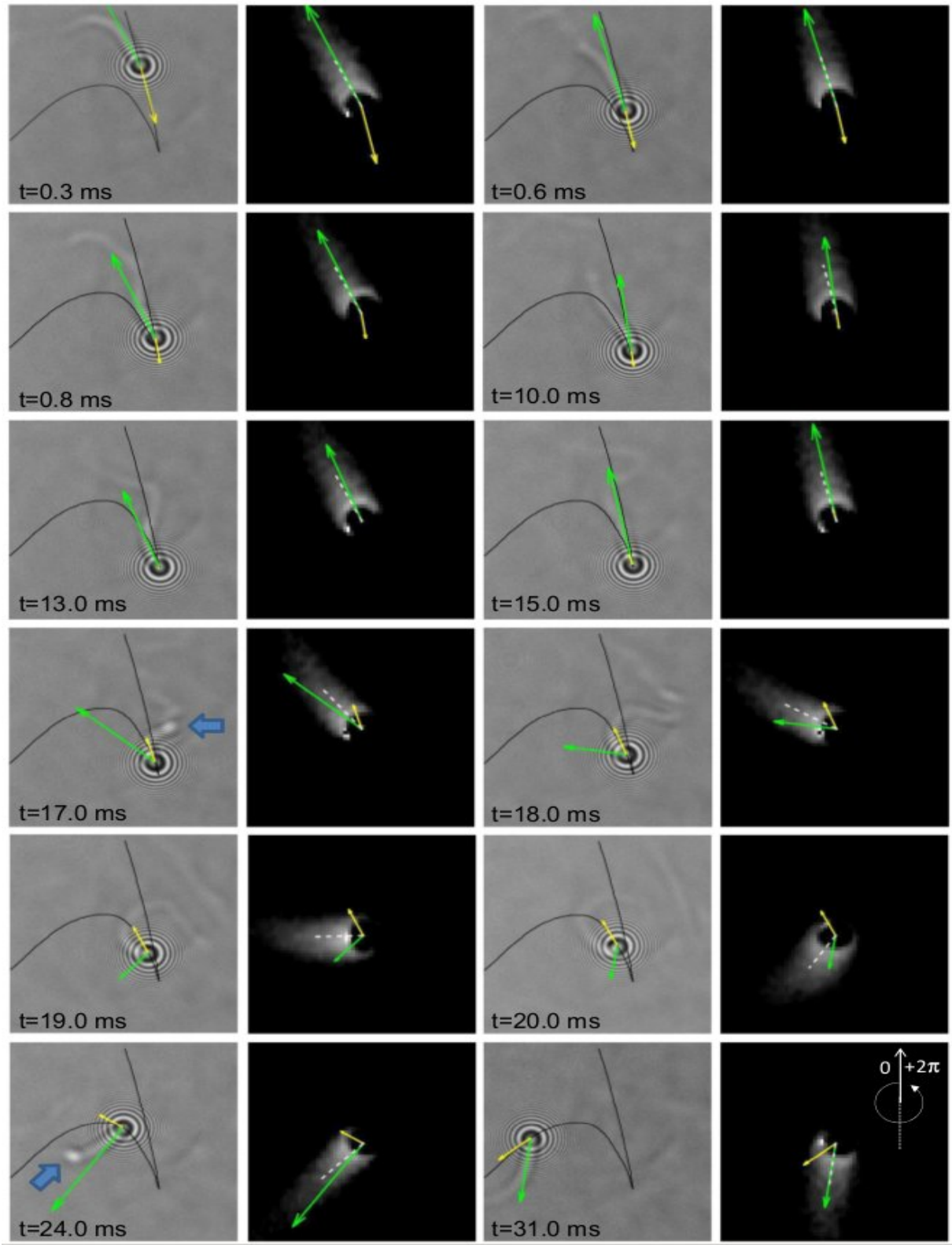

Fig 6 Images sample corresponding to droplet 2 trajectory. In gray (column 1 and 3): droplet hologram recorded on the CMOS after background correction; the black line is the trajectory of the droplet in the x – y plane; the yellow arrow is the velocity of the droplet (u_{xy}), the green one is the x – y Lagrangian relative velocity (ur_{xy}) calculated from the model. In black (column 2 and 4): the phase retrieved wake, magnified and centered on the droplet, with the same two velocities; the white dotted line materializes the axis of the wake; the two blue arrows point out the vapor releases.

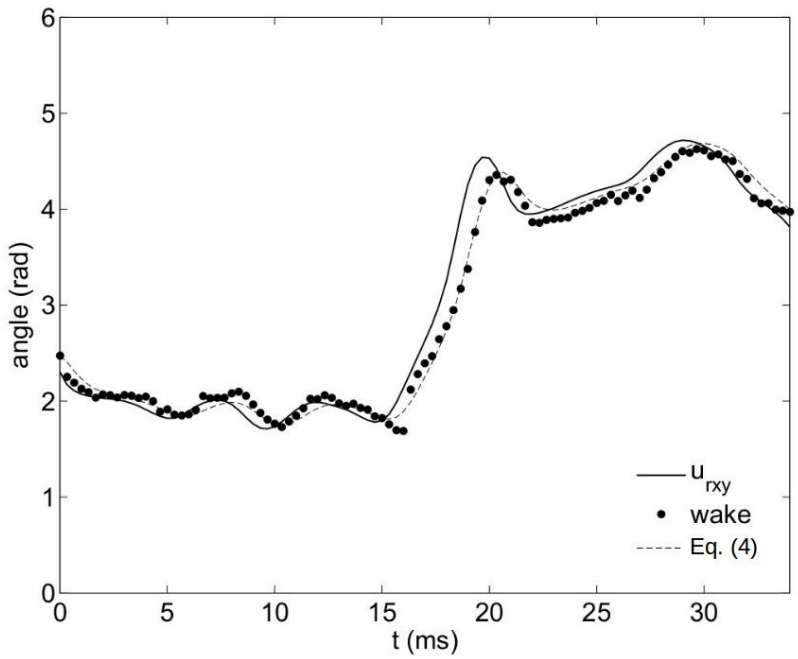

Fig 7 Comparison between the Lagrangian relative velocity ur_{xy} and the phase retrieved wake orientation in (x,y) plan.

5. Conclusion

Digital In-line holography was used to perform a Lagrangian tracking of droplets evaporating in an homogeneous and isotropic turbulence. An 'inverse problem' approach was used to reach the accuracy required by such a study, providing 3D trajectories and diameter estimation versus time. In addition, the wake of vapor around the droplets was reconstructed using a standard back light propagation method. This vapor wake orientation is found to be in very good agreement with the relative velocity, calculated from the IPA measurements and the droplets equation of motion, demonstrating the overall coherency of the procedure. Comparison of the measured diameter evolution with a simple evaporation/condensation model, previously validated on free falling configuration shows that the evaporation rate of droplets may be affected by the turbulent flow. In numerous cases (not all) the evaporation rate was no more constant as it was in laminar condition. Strong fluctuations of this rate were observed and it

seems that they are connected with fast variations of the relative velocity, in magnitude and orientation. However, further investigations and a larger amount of statistics are required to assess this assumption, to quantify the influence of turbulence on evaporation and to clearly explain the involving mechanisms.

Acknowledgements

This work was partially funded by the French National Research Agency (ANR) under grants AMO-COPS (ANR-13-BS09-0008-02) and TEC2 (ANR-12-BS09-0011).

References

Birouk M, Gökalp I (2006) Current status of droplet evaporation in turbulent flows. Prog Energ Combust Sci 32(4):408–423

Chareyron D, Marié JL, Fournier C, Gire J, Grosjean N, Denis L, Lance M, Méès L (2012) Testing an in-line digital holography "inverse method" for the Lagrangian tracking of evaporating droplets in homogeneous nearly isotropic turbulence. New J Phys 14, 043039.

Clift R, Grace JR, Weber ME (1978) Bubbles, Drops and Particles. Academic Press

Marié J L, Grojean N, Méès L, Seifi M, Fournier C, Barbier B and Lance M (2014), Lagrangian measurements of the fast evaporation of falling Diethyl Ether droplets using in-line digital holography and a high-speed camera, submitted to Experiments in Fluids.

Méès L, Grosjean N, Chareyron D, Marié JL, Seifi M, Fournier C (2013) Evaporating droplet hologram simulation for digital in-line holography setup with divergent beam. J Opt Soc Am A 30(10):2021–2028.

Michaelides E (2006) Particles, bubbles and drops: Their Motion, Heat and Mass Transfer. World Scientific.

Reveillon J, Demoulin FX (2007) Effects of the preferential segregation of droplets on evaporation and turbulent mixing. J Fluid Mech 583:273–302

Seifi M, Fournier C, Grosjean N, Méès L, Marié JL, Denis L (2013) Accurate 3D tracking and size measurement of evaporating droplets using an in-line digital holography and 'inverse problems' reconstruction approach. Opt Express 21(23), DOI: 10.1364/OE.21.027964.

Soulez F, Denis L, Fournier C, Thiébaut E, Goepfert C (2007a) Inverse-problem approach for particle digital holography: accurate location based on local optimization. J Opt Soc Am A 24(4):1164–1171.

Soulez F, Denis L, Thiébaut E, Fournier C, Goepfert C (2007b) Inverse problem approach in particle digital holography: outof-field particle detection made possible. J Opt Soc Am A 24(12):3708–3716.